JOURNAL OF SOLID STATE CHEMISTRY 139, 248–258 (1998)
ARTICLE NO. SC987837

Synthesis and Crystal Structure of a New Mixed-Valence Terbium Fluoride, $KTb^{III}Tb_2^{IV}F_{12}$, and Related $KLn^{III}M_2^{IV}F_{12}$ Compounds (M^{IV} = Tb, Zr, Hf; Ln^{III} = Ce–Lu)

Eric Largeau, Malika El-Ghozzi, and Daniel Avignant[1]

Laboratoire des Matériaux Inorganiques, Université Blaise Pascal, UPRES-A 6002 CNRS, 63177 Aubiere Cedex, France

Received November 25, 1997; in revised form March 24, 1998; accepted March 31, 1998

During a phase relationship study of the system KF–TbF_3–TbF_4, carried out using X-ray diffraction on samples synthesized under a fluorine atmosphere, a new mixed-valence terbium fluoride, KTb_3F_{12}, was brought out. Its crystal structure was determined from single-crystal X-ray diffraction data and refined to a conventional $R = 0.031$ ($R_w = 0.057$) for 920 independent reflections with $F > 4\sigma(F)$. It crystallizes in the tetragonal system with space group $I4/m$ (No. 87) and unit cell parameters $a = 7.715(1)$ Å, $c = 7.530(1)$ Å, $Z = 2$. The crystal-structure analysis revealed a perfect ordering between Tb^{3+} and Tb^{4+} cations. The structure is built of chains of edge-sharing $[TbF_8]^{4-}$ dodecahedra further linked by $[TbF_8]^{5-}$ cubes alternating along the [001] direction with K^+ ions in 12-coordination. A series of homologous compounds, $KLn^{III}M_2^{IV}F_{12}$ (M^{IV} = Tb, Zr, Hf; Ln = Ce–Lu), was also evidenced.

INTRODUCTION

Despite recent crystal structure studies related to tetravalent terbium fluorides (1–4), the IV oxidation state of this rare earth remains little known. This lack of information results from the difficulty in reaching this high oxidation state which can be achieved only under a high oxidizing atmosphere such as pure fluorine gas flow. Comparatively and inversely, the IV oxidation state of praseodymium is easier to achieve under oxygen rather than fluorine. As fluorine is the element of predilection to raise the IV oxidation state of terbium we used a dynamical fluorination process under pure fluorine gas flow to synthesize tetravalent terbium fluorides (1–8) among which some were obtained as single crystals (1–4).

At present it is well known that, on heating, terbium tetrafluoride, as a number of other fluorides of transition elements in their higher oxidation state, tends to decompose with elimination of fluorine according to the reaction TbF_4 (s) $\rightarrow TbF_3$ (s) + $\frac{1}{2}F_2$ (g). The decomposition temperature lies in the range 540–680°C according to Nikulin *et al.* (9) and around 450°C after Gibson and Haire (10). Despite the discrepancy between these values due to different experimental conditions, we hold that the thermal decomposition occurs even if the heat treatment of TbF_4 is carried out under pure fluorine gas at atmospheric pressure at about 580–650°C.

The thermal decomposition of terbium tetrafluoride can, however, be limited by a rapid recombination of both tetravalent and trivalent terbium fluorides to yield $TbF_{3.75}$ (Tb_4F_{15}). More generally the thermal decomposition of terbium tetrafluoride depends on the relative thermodynamical stabilities of the phases susceptible to be formed by recombination of the constituents brought together. This outstanding feature has been used to account for the synthesis of the original mixed-valence terbium fluoride KTb_3F_{12} ($KTb^{III}Tb_2^{IV}F_{12}$), which is the first representative of a new family of fluorides, $KLn^{III}M_2^{IV}F_{12}$ (M^{IV} = Tb, Zr, Hf; Ln^{III} = Ce–Lu).

This paper deals with the crystal structure determination of KTb_3F_{12} from single-crystal X-ray diffraction data, the synthesis of homologous compounds, and a discussion about the relationships between this structural type and β-$BaTbF_6$, $RbTh_3F_{13}$, and rutile structures.

EXPERIMENTAL

During a preliminary study of the system KF–TbF_4, carried out using X-ray diffraction, five well-defined compounds were mentioned, namely, K_3TbF_7, K_2TbF_6, $K_7Tb_6F_{31}$, $KTbF_5$, and KTb_2F_9 (5). Whereas the first four are perfectly white, the last is light brown and was obtained by heating at 500°C, under a pure fluorine gas flow, a mixture 1KF + 2TbF_4. From a single-crystal structure determination carried out very recently (11), this compound falsely reported as KTb_2F_9 is now known as $K_2Tb_4F_{17}$, e.g., $K_2Tb^{III}Tb_3^{IV}F_{17}$. Under the same conditions, the mixture IKF + 3TbF_4 leads to a diphasic composition involving

[1] To whom any correspondence should be addressed.

0022-4596/98 $25.00

$K_2Tb_4F_{17} + TbF_4$. If the temperature is raised to 650°C the first sample ($1KF + 2TbF_4$) always yields $K_2Tb_4F_{17}$, whereas the second ($1KF + 3TbF_4$) gives a new compound with formula KTb_3F_{12}, that is, $KTb^{III}Tb_2^{IV}F_{12}$. This result is perfectly understandable provided that $KTbF_5$ is the last stable intermediate compound occuring in the $KF–TbF_4$ system. Therefore for the $1KF–3TbF_4$ composition there is unreacted terbium tetrafluoride which decomposes on heating, yields TbF_3, and leads to the ternary $KF–TbF_3–TbF_4$ system where the KTb_3F_{12} is a stable phase (Fig. 1). Consequently, polycrystalline samples of KTb_3F_{12} were obtained by heating overnight at 650°C stoichiometric mixtures of the starting dehydrated KCl and TbF_4 in a nickel boat under pure fluorine atmosphere.

Light orange single crystals, suitable for a structural study, were obtained by annealing at 700°C for 48 h a mixture of composition $1KF–3TbF_4$. The X-ray powder diffraction pattern of crushed single crystals is identical to that of a polycrystalline sample of KTb_3F_{12} prepared in the solid state.

Polycrystalline samples of homologous fluorides $KLnZr_2F_{12}$ and $KLnHf_2F_{12}$ (Ln = Ce–Lu) were synthesized by heating twice at 500°C for 24 h a stoichiometric mixture of the starting fluorides $1KF + 1LnF_3 + 2ZrF_4$ (HfF_4). These new compounds do not melt congruently and decompose above approximately 560°C. Their crystal-chemical characteristics are gathered in Table 1. From this table, it can be seen that the cell parameters within the three series of phases (M^{IV} = Tb, Zr, Hf) as well as the cell volume increase smoothly as a function of the ionic radius of the rare earth. More worthy of note is that no representative of this structural family could have been obtained for La^{3+} and also Y^{3+} which often behaves as a rare earth from the crystal-chemical point of view (12). This result is discussed later, in the light of the crystal structure.

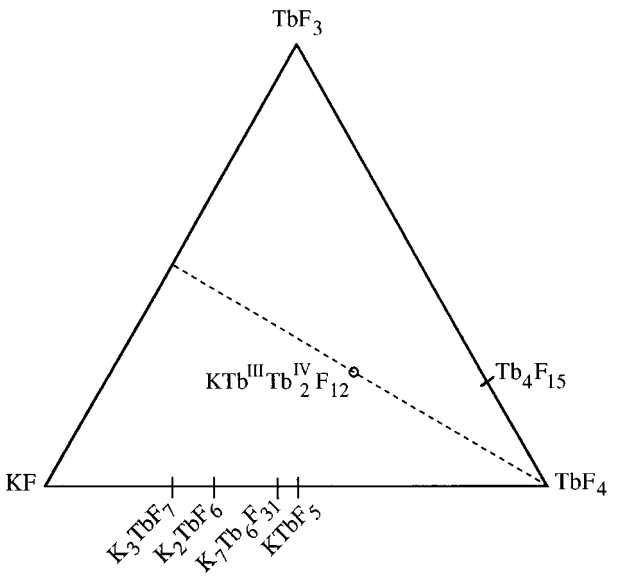

FIG. 1. Phase relationship in the $KF–TbF_3–TbF_4$ system.

TABLE 1
Cell Parameters and Cell Volume of $KLnM_2F_{12}$ Compounds Obtained from X-ray Powder Diffraction Data

	a (Å)	c (Å)	V (Å^3)
$KCeTb_2F_{12}$	7.807(4)	7.591(6)	462.7(5)
$KPrTb_2F_{12}$	7.795(4)	7.580(5)	460.6(5)
$KNdTb_2F_{12}$	7.780(8)	7.573(8)	458.4(8)
$KSmTb_2F_{12}$	7.753(4)	7.553(6)	454.0(5)
$KGdTb_2F_{12}$	7.730(6)	7.540(3)	450.5(5)
$KTbTb_2F_{12}$	7.716(7)	7.527(6)	448.1(7)
$KDyTb_2F_{12}$	7.713(6)	7.522(5)	447.5(6)
$KHoTb_2F_{12}$	7.701(4)	7.516(5)	445.7(4)
$KErTb_2F_{12}$	7.695(8)	7.511(6)	444.7(7)
$KTmTb_2F_{12}$	7.687(6)	7.502(7)	443.3(6)
$KYbTb_2F_{12}$	7.678(7)	7.497(8)	442.0(7)
$KLuTb_2F_{12}$	7.671(5)	7.489(5)	440.7(5)
$KCeZr_2F_{12}$	7.722(5)	7.461(6)	444.9(5)
$KPrZr_2F_{12}$	7.706(7)	7.448(7)	442.3(7)
$KNdZr_2F_{12}$	7.688(4)	7.434(9)	439.4(6)
$KSmZr_2F_{12}$	7.663(4)	7.411(7)	435.2(5)
$KGdZr_2F_{12}$	7.629(6)	7.391(7)	430.2(6)
$KTbZr_2F_{12}$	7.625(9)	7.381(6)	429.1(8)
$KDyZr_2F_{12}$	7.612(8)	7.375(4)	427.3(7)
$KHoZr_2F_{12}$	7.599(4)	7.363(5)	425.2(4)
$KErZr_2F_{12}$	7.587(6)	7.365(6)	423.9(6)
$KTmZr_2F_{12}$	7.582(4)	7.347(7)	422.4(5)
$KYbZr_2F_{12}$	7.567(7)	7.342(8)	420.4(7)
$KLuZr_2F_{12}$	7.562(5)	7.335(6)	419.4(5)
$KCeHf_2F_{12}$	7.708(6)	7.435(7)	441.7(6)
$KPrHf_2F_{12}$	7.694(4)	7.422(5)	439.4(4)
$KNdHf_2F_{12}$	7.675(9)	7.410(4)	436.5(8)
$KSmHf_2F_{12}$	7.648(4)	7.386(5)	432.0(4)
$KGdHf_2F_{12}$	7.619(8)	7.364(6)	427.5(7)
$KTbHf_2F_{12}$	7.607(6)	7.353(7)	425.5(6)
$KDyHf_2F_{12}$	7.595(4)	7.345(8)	423.7(6)
$KHoHf_2F_{12}$	7.583(6)	7.336(4)	421.8(5)
$KErHf_2F_{12}$	7.571(4)	7.328(6)	420.0(5)
$KTmHf_2F_{12}$	7.563(3)	7.319(5)	418.6(4)
$KYbHf_2F_{12}$	7.551(7)	7.311(8)	416.9(7)
$KLuHf_2F_{12}$	7.546(5)	7.306(4)	416.0(5)

STRUCTURE DETERMINATION AND REFINEMENT

Single-crystal X-ray diffraction intensities were collected with an Enraf–Nonius CAD4 four-circle diffractometer under conditions listed in Table 2. An empirical absorption correction, deduced from psi-scan series on 204, $00\bar{4}$, $\bar{1}1\bar{4}$, $\bar{1}3\bar{6}$, $\bar{2}1\bar{3}$, and $01\bar{5}$ reflections, was applied to all data.

K and Tb atomic positions were determined from the Patterson function and refined first in the centrosymmetric $I4/mmm$ space group. Then two independent fluorine atoms were located from a difference Fourier synthesis. Refinements

TABLE 2
Crystallographic Data and Data Collection Parameters for KTb_3F_{12}

Chemical formula	KTb_3F_{12}
Fw	743.85 g
Symmetry	Tetragonal
Space group	*I*4/*m* (No. 87)
Unit cell parameters	
a	7.715(1) Å
c	7.530(1) Å
V	448.3(1) Å^3
Z	2
ρ_{calc} (g cm^{-3})	5.513(1)
Data collection temperature	293 K
Crystal size	$0.03 \times 0.03 \times 0.02$ mm
Radiation	Mo$K\alpha$ ($\lambda = 0.71069$ Å) graphite monochromated
μ (Mo$K\alpha$)	24.59 mm^{-1}
Transmission factors	0.746–0.996
Scan mode	ω–2θ
Scan width	$(0.80 + 0.35 \tan\theta)^\circ$
Scan aperture	$(2.70 + 0.40 \tan\theta)$ mm
θ range	$1^\circ \le \theta \le 45^\circ$
Index ranges	$0 \le h \le 15, 0 \le k \le 15, 0 \le l \le 15$ $-15 \le h \le 0, -15 \le k \le 0,$ $-15 \le l \le 0$
Period of intensity control	3600 s, $\sigma = 0.02$
Number of measured reflections	2132
Number of independent reflections	966, $R_{int} = 0.06$
Observed reflections with $F > 4\sigma(F)$	920
Number of variables	24
Weighting scheme	$w = 1/(\sigma^2(F_0^2) + (0.0135 \times P)^2 + 5.07 \times P$ $P = (\mathrm{Max}(F_0^2, 0) + 2F_c^2)/^3)$
Secondary extinction parameter	0.00737(9)
R, R_w	0.031, 0.057
Goodness of fit	$s = 1.070$
Maximum and minimum electron density in final difference Fourier synthesis	4.51 *e* Å^{-3} close to Tb^{IV} -3.32 *e* Å^{-3} close to Tb^{III}

of the atomic coordinates and anisotropic thermal parameters including a secondary extinction parameter resulted in a conventional $R = 0.024$ ($R_w = 0.028$). The atomic scattering factors for the ions and the anomalous dispersion terms were taken from the International Tables for X-ray Crystallography (13). As no scattering factors were available for the Tb^{4+} ion, we used those of the isoelectronic Gd^{3+} one.

According to this description of the structure in the *I*4/*mmm* space group one crystallographically independent fluorine atom was located on the 16*n* site but exhibited a high thermal parameter. A more satisfactory result was obtained by describing this position by the 32*o* site, half occupied. But in the light of the neutron diffraction experiment the symmetry had to be lowered to *I*4/*m* and a twin was evidenced.

TABLE 3
Atomic Coordinates and Thermal Parameters for KTb_3F_{12}

Atoms	Wyckoff position	Occupancy factor	*x*	*y*	*z*	U_{eq} (Å^2)
K	2*a*	1.0	0	0	0	0.0189(4)
Tb^{III}	2*b*	1.0	0	0	1/2	0.00629(7)
Tb^{IV}	4*d*	1.0	0	1/2	1/4	0.00537(6)
F(1)	8*h*	1.0	0.3455(4)	0.020(1)	0	0.015(1)
F(2)	16*i*	1.0	0.2377(3)	0.0335(3)	0.6800(3)	0.017(1)

Anisotropic thermal parameters (Å$^2 \times 10^3$)[a]

	U_{11}	U_{22}	U_{33}	U_{12}	U_{13}	U_{23}
K	17.5(5)	U_{11}	2.19(7)	0	0	0
Tb^{III}	6.2(1)	U_{11}	6.5(1)	0	0	0
Tb^{IV}	5.68(7)	U_{11}	4.75(8)	0	0	0
F(1)	9(1)	29(4)	9(1)	0	0	0.1(9)
F(2)	11(1)	26(2)	13(1)	$-0.2(1)$	$-0.3(1)$	$-0.3(1)$

[a] The form of the anisotropic displacement parameters is

$$\exp[-2\pi^2(h^2a^{*2}U_{11} + k^2b^{*2}U_{22} + l^2c^{*2}U_{33} + 2hka^*b^*U_{12} + 2hla^*c^*U_{13} + 2klb^*c^*U_{23})].$$

The description of the cationic network in the *I*4/*m* space group is exactly the same as in the *I*4/*mmm* space group, and the lowering of the symmetry is due only to the F(2) position. Using the TWIN and BASF options of SHELXL97, the weight of each individual was found to be very close to 0.5. The final refinement resulted in $R = 0.031$ ($R_w = 0.057$) for 920 reflections. Final positional and thermal parameters are given in Table 3. A bond valence analysis of the structure (Table 4) confirmed the existence of the oxidation states +III and +IV for Tb. These calculations were performed according to Brese and O'Keeffe's method (14) by using the relation $v_{ij} = \exp[(R_{ij} - d_{ij})/b]$, where v_{ij} is the valence of a bond between *i* and *j* atoms, d_{ij} the distance between these atoms, *b* a "universal" constant equal to 0.37 Å, and R_{ij} the bond-valence parameter. This last value was evaluated to 1.905 Å for the Tb^{IV}–F bond (3) and 1.936 for the Tb^{III}–F bond (14).

The main interatomic distances are listed in Table 5. All computer programs used for data collection and reduction

TABLE 4
Bond Valence Analysis of the KTb_3F_{12} Structure

Atoms	Coordination	K	Tb^{III}	Tb^{IV}	F(1)	F(2)	v_{ij} calc	v_{ij}th
K	4F(1) + 8F(2)				0.159 (×4)	0.059 (×8)	1.11	1
Tb^{III}	8F(2)					0.379 (×8)	3.03	3
Tb^{IV}	4F(1) + 4F(2)				0.413 (×4)	0.581 (×4)	3.98	4
F(1)	$2Tb^{IV} + 1K$	0.159		0.413 (×2)			0.99	1
F(2)	$1Tb^{IV} + 1K + 1Tb^{III}$	0.059	0.379	0.581			1.02	1

TABLE 5
Selected Distances (Å) in KTb_3F_{12}

	Tb^{IV}–F(1)	2.107(2) (×4)	
	Tb^{IV}–F(2)	2.223(2) (×4)	
	$\langle Tb^{IV}-F\rangle = 2.170$ Å		
	Tb^{III}–F(2)	2.295(3) (×8)	
	K–F(1)	2.670(3) (×4)	
	K–F(2)	3.039(2) (×8)	
	$\langle K-F\rangle = 2.916$ Å		
K–Tb^{III}	3.7652(1)	K–Tb^{III}	5.4556(1)
K–Tb^{IV}	4.2926(1)	Tb^{IV}–Tb^{III}	4.2926(1)
Tb^{IV}–Tb^{IV}	3.7652(1)	Tb^{IV}–Tb^{IV}	5.4556(1)

were issued from the SDP (15), and the refinement was performed with SHELXL 97 (16). A list of the observed and calculated structure factors may be obtained from the authors, on request.

STRUCTURE DESCRIPTION AND DISCUSSION

In the title compound, as in other tetravalent terbium fluorides (1, 3, 4), the Tb^{4+} ions are surrounded by eight fluoride ions delimiting a slightly distorted dodecahedron. Two sets of four fluorine atoms form the classical trapezoids $F(2)^a$–$F(1)^b$–$F(1)^c$–$F(2)^d$ and $F(2)^e$–$F(1)^f$–$F(1)^g$–$F(2)^h$ (Fig. 2) constitutive of a dodecahedron (17). The average Tb^{IV}–F distance (2.170 Å) is in good agreement with the mean distances (2.17–2.18 Å) already mentioned for 8-coordinated Tb^{4+} (1–4). The Tb^{IV}–F distances are more regular (2.092–2.226 Å) than those encountered in analogous $[TbF_8]^{4-}$ dodecahedra, namely, in β-$BaTbF_6$ (2.081–2.271 Å) (1), α-$BaTbF_6$ (2.10–2.45 Å) (2), $KTbF_5$ (2.018–2.293 Å) (3), and $CsTbF_5$ (2.059–2.255 Å) (4), the crystal structures of which have been refined from single-crystal X-ray diffraction data.

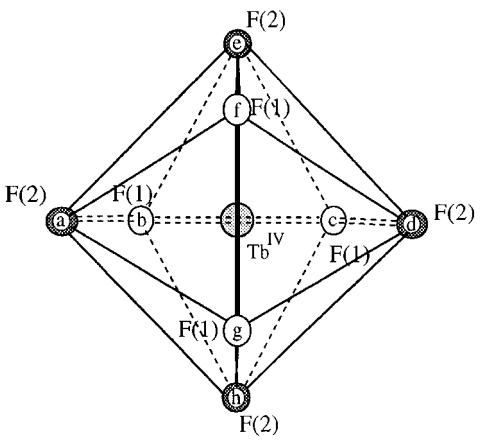

FIG. 2. View along [001] of the $[Tb^{IV}F_8]^{4-}$ dodecahedron.

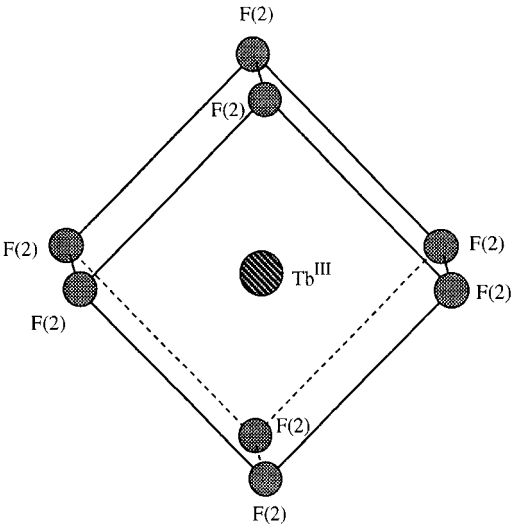

FIG. 3. View along [001] of the $[Tb^{III}F_8]^{5-}$ slightly distorted cube.

The trivalent terbium atom lies at the center of an almost regular cube built of eight F(2) fluorine atoms (Fig. 3). Such a coordination polyhedron has already been evidenced for a part of the Ho atoms in KHo_2F_7 (18).

The potassiums are surrounded by 12 fluoride ions, namely, four F(1) and eight F(2) (Fig. 4).

The three-dimensional structure is built of infinite chains of edge-sharing $[Tb^{IV}F_8]^{4-}$ dodecahedra running along the *c* direction (Fig. 5). The alternated F(1)–F(1) shared edges in these chains are orthogonal. These chains are further linked together by $[Tb^{III}F_8]^{5-}$ slightly distorted cubes by sharing corners. These $[TbF_8]^{5-}$ cubes alternate along the *c* direction with cavities encompassing the K^+ ions (Figs. 6 and 7) which are 12-coordinated by the fluoride ions (Fig. 4).

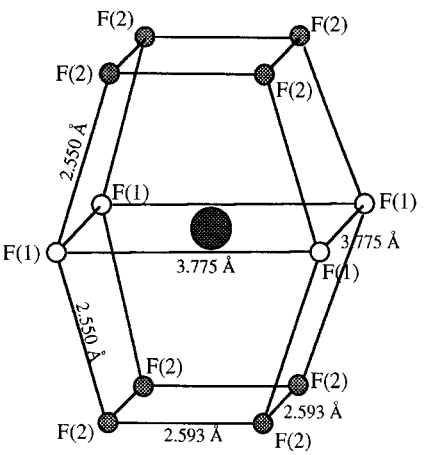

FIG. 4. Perspective view of the potassium coordination polyhedron in KTb_3F_{12}.

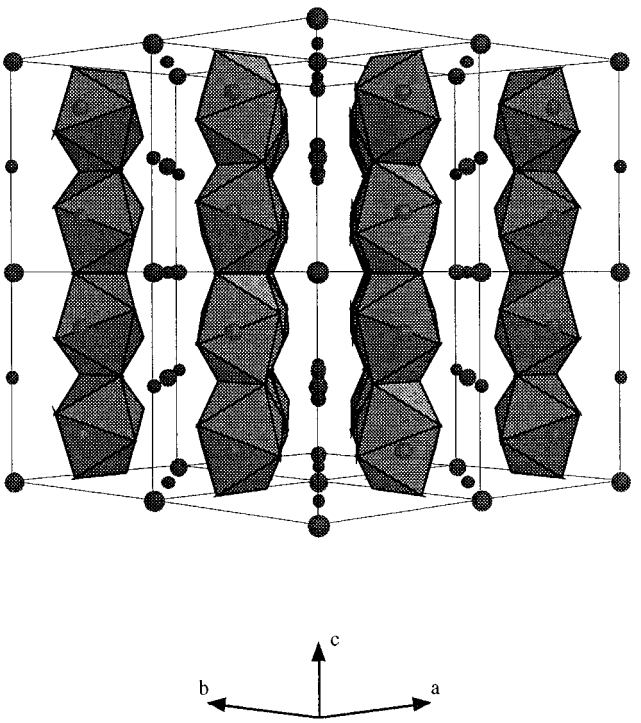

FIG. 5. Isolated chains of edge-sharing dodecahedra viewed along the [110] direction.

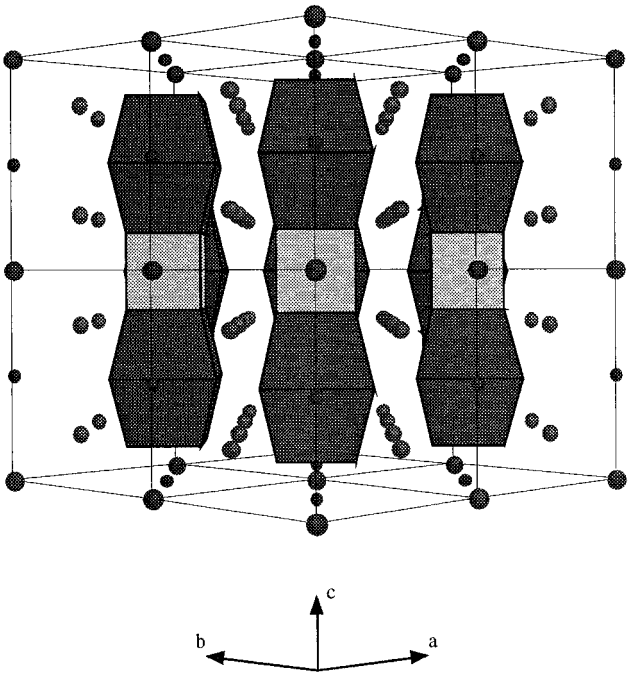

FIG. 7. Columns of alternated $[Tb^{III}F_8]^{5-}$ cubes and $[KF_{12}]^{11-}$ polyhedra.

We have already mentioned under Experimental that no representative of this structural family could have been obtained for La^{3+} and Y^{3+}. These observations may be explained as follows. In this $KA^{III}B^{IV}F_{12}$ structural type the trivalent cation A lies on the 2*b* site of the $I4/m$ space group and is surrounded by eight fluorine ions. Therefore the 8-coordination polyhedron exhibits the $4/m$ or C_{4h} symmetry. It should be remembered that *f* orbitals may also be used in the formation of covalent bonds in compounds that are predominantly ionically bonded (19). Using Kimball's method (20) to determine the hybridization of the cationic atomic orbitals, the eight-dimensional reducible representation $\Gamma_h = A_g + B_g + E_g + A_u + B_u + E_u$ was obtained for C_{4h} symmetry. There is no odd orbital among *p* orbitals which serves as a basis for the B_u irreducible representation of the C_{4h} group. So, to form a set of eight equivalent σ bonds with appropriate transformation properties from atomic orbitals it is necessary to select one *f* function out of two possible that may generate the B_u representation as do the σ functions. To strengthen this assumption, the synthesis of the $KBiZr_2F_{12}$ compound has been undertaken and resulted also in a tetragonal phase with $a = 7.640(3)$ Å and $c = 7.411(3)$ Å, isotypic with KTb_3F_{12}. Therefore, cations such as La^{3+} and Y^{3+} with ionic radii of appropriate sizes but with empty *f* orbitals do not lead to $KA^{III}B_2^{IV}F_{12}$ compounds, whereas Bi^{3+} with full 4*f* orbitals does.

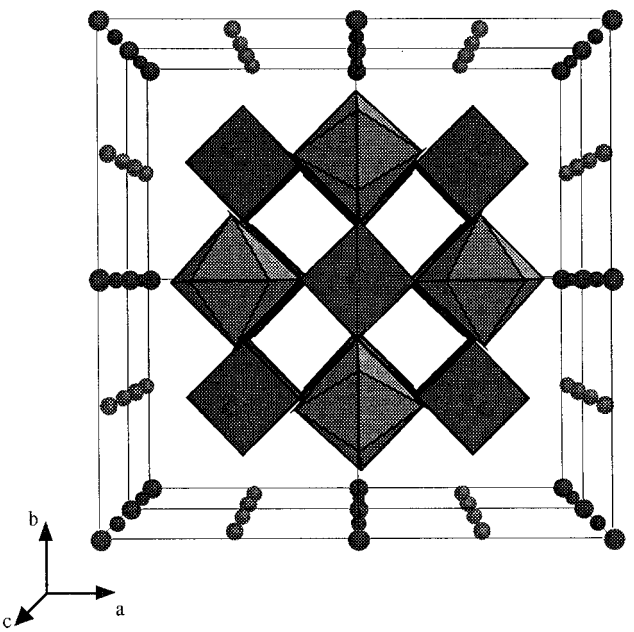

FIG. 6. Projection of $[Tb^{IV}F_6]_n^{2n-}$ chains connected by $[Tb^{III}F_8]^{5-}$ cubes along [001].

RELATIONSHIPS WITH OTHER STRUCTURES

For particular stoichiometries, namely, $2MF$–$1MF_4$ or $1MF_2$–$1MF_4$, several fluorides adopt a structure that is built of isolated chains of 8-coordination polyhedra.

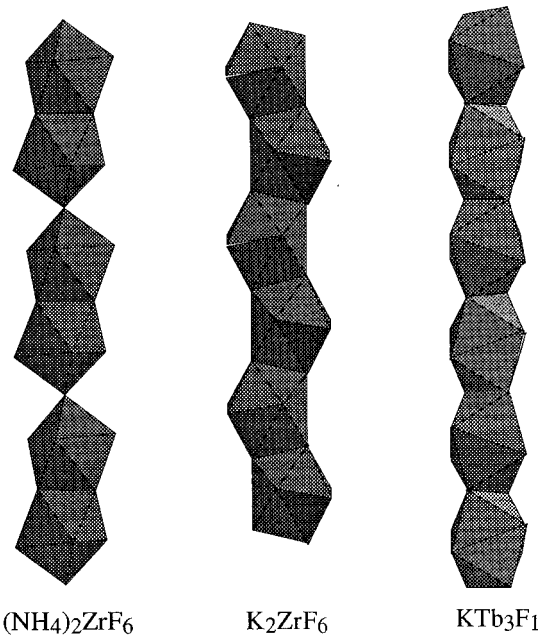

FIG. 8. Examples of $[MF_6]_n^{2n-}$ chains built up from $[MF_8]^{4-}$ polyhedra.

Different chains can be formed depending on the geometry of the polyhedra and their linkage. Three types of $[MF_6]_n^{2n-}$ chains built up from $[MF_8]^{4-}$ polyhedra are frequently found:

The first type exists in γ $BaZrF_6$ (21) and $(NH_4)_2ZrF_6$ (22). The chains are built of bicapped trigonal prisms linked alternatively by faces and corners (Fig. 8). Barium and ammonium ions respectively provide the cohesion of the three-dimensional structures.

The second type is encountered in K_2ZrF_6 (23) and related structures and characterized by chains built up from edge-sharing distorted dodecahedra (Fig. 8). If we consider that such a polyhedron is built of two sets of anions forming the trapezoids $F(2)^a$–$F(1)^b$–$F(1)^c$–$F(2)^d$ and $F(2)^e$–$F(1)^f$–$F(1)^g$–$F(2)^h$ (Fig. 1), the shared edges involve F(1)–F(2) and are ideally parallel to each other in a regular polyhedron.

The third type of $[MF_6]_n^{2n-}$ chains, very common, is present in KTb_3F_{12} and in β-$BaTbF_6$ (1). The chains are also built of edge-sharing dodecahedra; however, the common edges are ideally orthogonal to each other and involve alternatively $F(1)^b$–$F(1)^c$ and $F(1)^f$–$F(1)^g$ (Fig. 2).

It is worth noting that both β-$BaTbF_6$ and KTb_3F_{12} structures are built up of similar chains of edge-sharing $[TbF_8]^{4-}$ dodecahedra and differ only by their relative arrangement. A simple structural relationship between these two structural types can be evidenced by considering β-$BaTbF_6$ (written β-$Ba_2Tb_2F_{12}$ for convenience), viewed along the [100] direction and KTb_3F_{12} projected down [001] (Fig. 9). Then, the structure of the former is built of chains that are connected by Ba^{2+} cations, whereas in $KTb^{III}Tb_2^{IV}F_{12}$, the slightly distorted chains are linked by

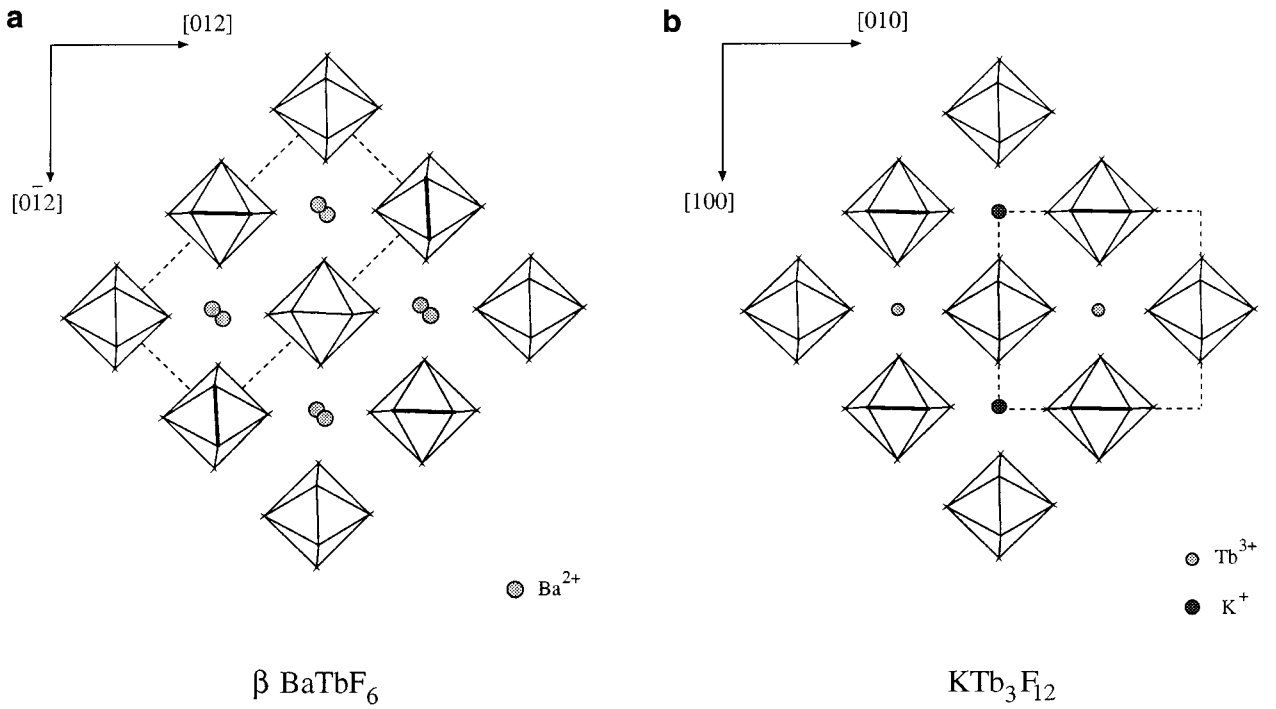

FIG. 9. Relationship between structures of β-$BaTbF_6$ and KTb_3F_{12}. (a) Projection of the structure of β-$BaTbF_6$ along [100]. (b) Projection of the structure of KTb_3F_{12} along [001].

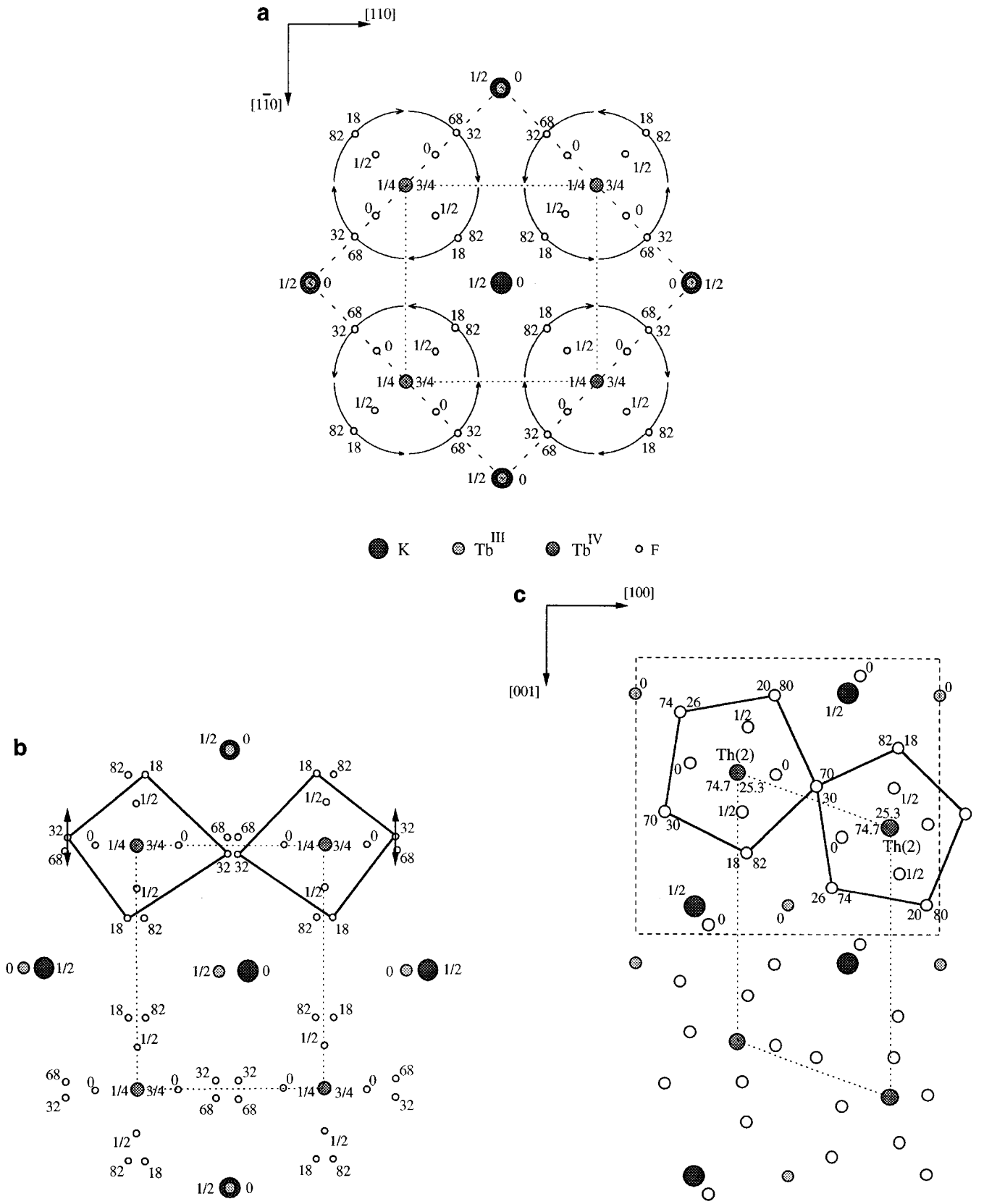

FIG. 10. Scheme of transformation of the KTb_3F_{12} structure (a) into the $RbTh_3F_{13}$ structure (c). Dashed lines: unit cells of KTb_3F_{12} and $RbTh_3F_{13}$. Dotted lines: 4^4 tetravalent cation network.

alternating Tb^{3+} and K^+ cations. In both structures, each chain has four nearest-neighbor chains. In KTb_3F_{12}, within these four chains, the shared edges lying in the same plane are parallel to each other and alternately to [010] and [100] directions. In β-$BaTbF_6$, the shared edges lying in the same plane are alternately orthogonal and parallel to [012] and [0$\bar{1}$2] directions, respectively. Consequently, the KTb_3F_{12} structure exhibits two different sites of 8- and 12-coordination, respectively, for Tb^{3+} and K^+, whereas in β-$BaTbF_6$ there is only one environment for 10-coordinated Ba^{2+}. The β-$BaTbF_6$ and KTb_3F_{12} structures may be related to each other. Starting from the β-$BaTbF_6$ structure, the KTb_3F_{12} structure may be obtained by rotation of $\pi/2$ one chain out of two around the [100] direction or by translation of $\mathbf{a}/2$ one chain relative to the other and by substituting in an ordered way the $Tb^{3+} + K^+$ couple for two Ba^{2+} ions. Conversely, the β-$BaTbF_6$ structure may be deduced from the KTb_3F_{12} structure by rotation of $\pi/2$ one chain out of two or by translation of $\mathbf{c}/2$ one chain relative to the other and by substitution of two Ba^{2+} for the couple $K^+ + Tb^{3+}$.

Another structural relationship can be envisaged between KTb_3F_{12} and $RbTh_3F_{13}$ (24). This latter phase contains two crystallographically independent thorium atoms in 9-coordination. One kind of thorium polyhedra, namely, $[Th(2)F_9]^{5-}$, by sharing orthogonal opposite edges, forms infinite chains which are further linked together by sharing vertices to form corrugated layers. These layers are held together by Th(1) and Rb atoms. Then, Tb^{IV} and Th(2), Tb^{III} and Th(1), and K and Rb play respectively similar roles in their own structure. The analogy is particularly obvious if the atomic positions are compared. As illustrated in Fig. 10, the $RbTh_3F_{13}$ structure can be deduced from the KTb_3F_{12} structure by alternated rotations of 45° of the anionic positions around the Tb^{IV} atoms (Fig. 10a). Such a rotation leads to the connection through corners of the $[TbF_6]_n^{2n-}$ chains (Fig. 10b) built of edge-sharing $(TbF_8)^{4-}$ dodecahedra. Then, a further insertion of one fluorine atom per cation which is achieved by the transformation of a common vertex into a shared edge results in the 9-coordination of the cation with a 2–5–2-like $[ThF_9]^{5-}$ polyhedron (Fig. 10c).

The KTb_3F_{12} (MX_3) structure may also be regarded as deriving from the rutile (MX_2) by insertion of an excess of anions. For this purpose a double-rutile unit cell is taken into account. Let us consider both structures viewed along the [001] direction with the origin of the double-c-rutile cell translated of $\mathbf{c}/4$. Then the cationic positions are similar as shown in Fig. 11. The mechanism corresponding to the transformation of the rutile structure into the KTb_3F_{12} structure can be formally decomposed in two steps (Fig. 12):

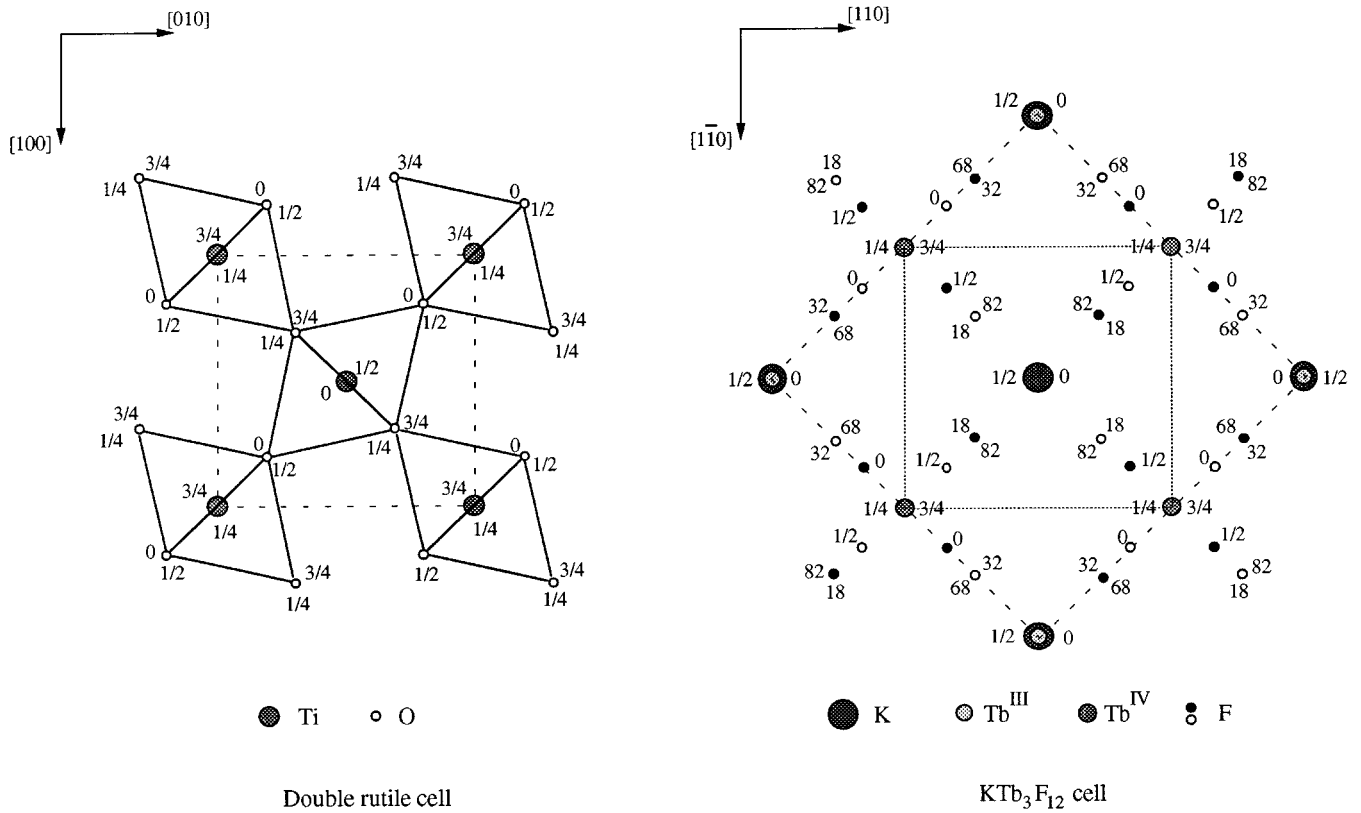

FIG. 11. Projection of the KTb_3F_{12} and rutile structures down [001] showing analogies between atomic positions.

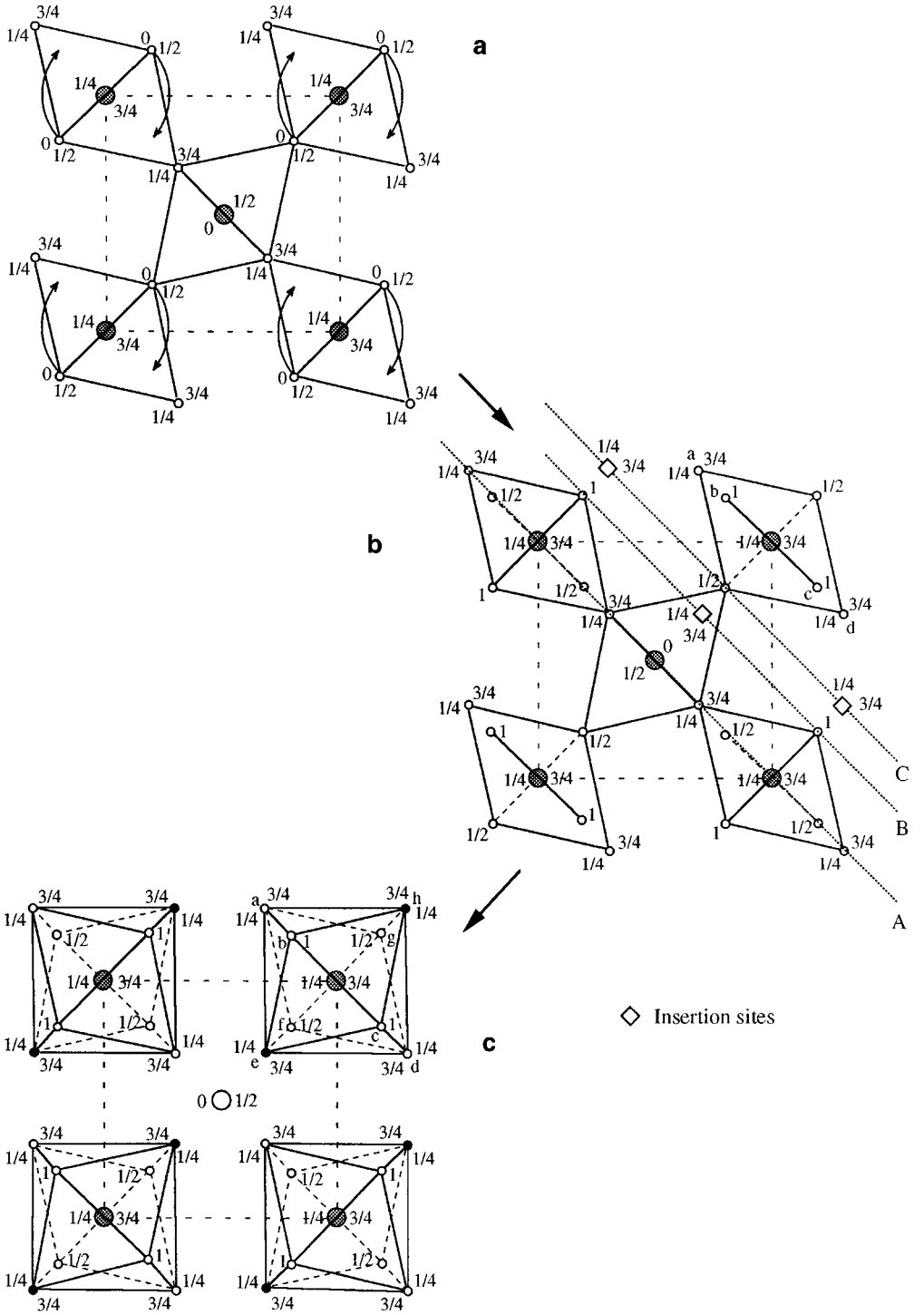

FIG. 12. Scheme showing the relationship between the rutile structure and the KTb_3F_{12} structure.

Rotation of all anions lying in $z = 0$ for one rutile chain and those lying in $z = 0.50$ for the adjacent chains (Fig. 12a). Thus, one trapezoid (*a–b–c–d*) existing in a dodecahedron is obtained.

Densification of two anionic planes. Actually, the preceding rotation leads to the formation of three atomic planes, parallel to $(\bar{1}10)$, called *A*, *B* and *C* in Fig. 12b. According to the Schläfli symbolism modified by Cundy

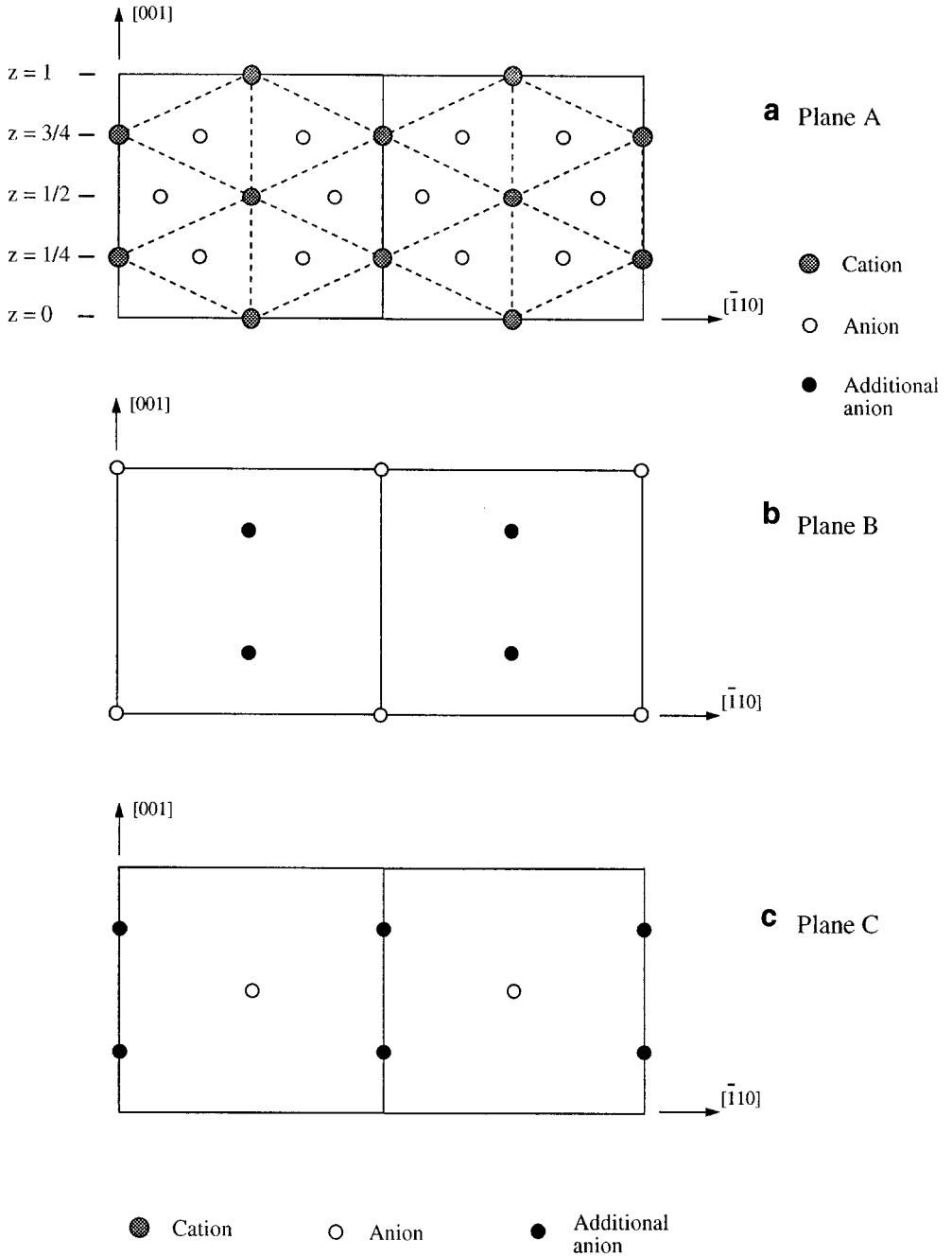

FIG. 13. View of the atomic planes accommodating the anionic excess in KTb_3F_{12} structure.

and Rollet (25), the first plane is constituted by a 3^6 cation network and hexagons of anions (Fig. 13a), whereas both B and C planes can be described as 4^4 anionic nets. The introduction in these two last planes of one anion per cation (black circles on Figs. 12c, 13b, and 13c) in vacancies changes the stoichiometry from MX_2 to MX_3 and results in the formation of the second trapezoid (*e–f–g–h* in Fig. 12). It is worth noting that such a densification transforms the B and C planes in identical $[3^2 \cdot 6^2] \cdot [3 \cdot 6 \cdot 3 \cdot 6]$ plane nets translated relative to each other of $a(\mathbf{a}/2 + \mathbf{b}/2 + \mathbf{c}/2)$.

Then, the anionic relaxation leads to a slight distortion of the plane nets observed in KTb_3F_{12}.

At present the determination of the magnetic structure of KTb_3F_{12} is in progress and the magnetic properties of members of this large family are also currently under investigation.

REFERENCES

1. E. Largeau, M. El-Ghozzi, J. Métin, and D. Avignant, *Acta Crystallogr. Sect. C* **53,** 530 (1997).
2. E. Largeau, V. Gaumet, M. El-Ghozzi, D. Avignant, and J. C. Cousseins, *J. Mater. Chem.* **7,** 1881 (1997)
3. V. Gaumet, E. Largeau, and D. Avignant, *Eur. J. Solid State Inorg. Chem.* **34,** 1075 (1997).
4. V. Gaumet and D. Avignant, *Acta Crystallogr. Sect. C* **53,** 1176 (1997).
5. D. Avignant and J. C. Cousseins, *C.R. Acad. Sci. C* **278,** 613 (1974).
6. M. Guillot, M. El-Ghozzi, D. Avignant, and G. Ferey, *J. Solid State Chem.* **97,** 400 (1992).
7. E. Largeau and M. El-Ghozzi, *J. Fluorine Chem.* **89,** 223 (1998).
8. D. Avignant, *Thesis*, University of Clermont Ferrand (1978).
9. V. V. Nikulin, S. A. Goryachenkov, M. V. Korobov, Y. M. Kiselev, and L. N. Sidorov. *Russ. J. Inorg. Chem.* **30,** 1441 (1985).
10. J. K. Gibson and R. G. Haire, *J. Solid State Chem.* **73,** 524 (1988).
11. E. Largeau, personnal communication.
12. S. Siekierski, *J. Solid State Chem.* **37,** 279 (1981).
13. "International Tables for X-ray Crystallography," Vol. IV. Kynoch Press, Birmingham, 1968.
14. N. E. Brese and M. O'Keeffe, *Acta Crystallogr. Sect. B* **47,** 192 (1991).
15. B. A. Frenz, *in* "Computing in Crystallography" (H. Shenk, R. Olthof–Hazekamp, H. Van Koningsveld, and G. C. Bassi, Eds.). Delft, 1982.
16. G. M. Sheldrick, "Crystallographical Computing 3" (G. M. Sheldrick, C. Krüger, and R. Goddard, Eds.), p. 175. Oxford Univ. Press, London, 1985.
17. M. A. Porai-Koshits and L. A. Aslanov, *J. Struct. Chem.* **13,** 244 (1972).
18. Y. Le Fur, S. Aléonard, M. F. Gorius, and M. Th. Roux, *Acta Crystallogr. Sect. B* **38,** 1431 (1982).
19. J. C. Eisenstein, *J. Chem Phys.* **25,** 142 (1956).
20. G. E. Kimball, *J. Chem. Phys.* **8,** 188 (1940).
21. A. Le Bail and A. M. Mercier, *J. Solid State Chem.* **101,** 229 (1992).
22. A. Zalkin, D. Eimerl, and S. P. Velsko, *Acta Crystallogr. Sect. C* **44,** 2050 (1988).
23. R. Hoppe and B. Mehlhorn, *Z. Anorg. Allg. Chem.*, **425,** 200 (1976).
24. G. Brunton, *Acta Crystallogr. B* **27,** 1823 (1971).
25. H. M. Cundy and A. P. Rollet, "Mathematical Models," 2nd ed., Clarendon Press, Oxford, 1961.